Differences in the reactivity of ammonium salts with methylamine

Yongchun Liu, Chong Han, Chang Liu, Jinzhu Ma, Qinxing Ma, Hong He

Research Center for Eco-Environmental Sciences, Chinese Academy of Sciences, Beijing, 100085, China

Correspondence to: Hong He (honghe@rcees.ac.cn)

Abstract

The heterogeneous uptake of methylamine (MA) onto $(NH_4)_2SO_4$, NH_4HSO_4, NH_4NO_3 and NH_4Cl was investigated using a Knudsen cell reactor coupled to a quadrupole mass spectrometer, *in situ* Raman spectrometer and theoretical calculations. Exchange reactions were observed between MA and NH_4NO_3, $(NH_4)_2SO_4$, and NH_4Cl were observed at 298 K. Simple acid-base reaction for MA was found taking place on NH_4HSO_4. $CH_3NH_3NO_3$ and CH_3NH_3Cl are not stable at low pressure and have higher dissociation vapor pressure than methylammonium sulfate. The observed uptake coefficients of MA on $(NH_4)_2SO_4$, NH_4HSO_4, NH_4NO_3 and NH_4Cl at 298 K were measured to be $6.30 \pm 1.03 \times 10^{-3}$, $1.78 \pm 0.36 \times 10^{-2}$, $8.79 \pm 1.99 \times 10^{-3}$ and $2.29 \pm 0.28 \times 10^{-3}$, respectively. A linear free energy relationship was found for the heterogeneous reactions between MA and NH_4Cl, $(NH_4)_2SO_4$ and NH_4NO_3. Namely, the natural logarithm of uptake coefficients of MA on these ammonium salts is linearly related to the electrostatic potential of the H atom in the NH_4^+ group.

1. Introduction

Recent field measurements suggest that organic nitrogen species may be an appreciable fraction of organic aerosol mass (Beddows et al., 2004; Chen et al., 2010; Pratt et al., 2009; Smith et al., 2010; Wang et al., 2010b). Amines are an important class of organic nitrogen species, and are frequently detected in aerosols, rainwater, and fog water (Ge et al., 2011a). They are emitted into the atmosphere from a variety of sources including livestock, biomass burning, sewage treatment, meat cooking, automobiles, industrial processes, and marine organisms (Ge et al., 2011b). The typical atmospheric concentration of alkylamines is < 1-14 nmol $N \cdot m^{-3}$, compared with ~25 ppbv of ammonia (Cornell et al., 2003). Recently, sources and sinks of atmospheric amines have received significant attention due to their potential toxicity to humans (Gong et al., 2004), their influence on atmospheric nitrogen cycle (Cornell et al., 2003) and their possible contribution to new particle formation (Smith et al., 2010; Wang et al., 2010a).

Smith et al. (2010) found that aminium salts accounted for 23% and 47% of the observed new particle formation in Hyytiälä in 2006 and Tecamac in 2007, respectively. With a class of strong bases, the gaseous alkylamines may undergo acid-base reactions with acids such as H_2SO_4 and HNO_3 to form salt particles. For example, Murphy et al. (2007) observed rapid particle nucleation when amines were injected into a chamber containing gaseous nitric acid. Wang et al. (2010b) also measured the obvious uptake of methylamine (MA), dimethylamine (DMA), and trimethyamine (TMA) into 59-82 wt% H_2SO_4. The uptake coefficients of these amines into H_2SO_4 are in the range of 2.0×10^{-2} - 4.4×10^{-2}. Some amines, such as TMA and triethylamine (TEA), also significantly contribute to secondary organic aerosol formation by NO_3 (Silva et al., 2008), OH or O_3 oxidation (Murphy et al., 2007; Gai et al., 2010). In addition, Wang et al. (2010c) proposed that a Mannich reaction

between amines and carbonyl compounds probably leads to the formation of nitrogen containing species with high molecular weight in secondary organic aerosols.

In field measurements, alkylamines are usually internally mixed with sulfate and nitrate ions in aerosols (Facchini et al., 2008; Pratt et al., 2009; Smith et al., 2010). It should be noted, however, that ambient ammonia concentrations tend to be an order of magnitude greater than amine concentrations (Murphy et al., 2007), and the uptake coefficient of ammonia by H_2SO_4, approximately 1 (Liggio et al., 2011; Shi et al., 1999; Swartz et al., 1999), is also one or two orders of magnitude greater than that of amine. Conversely, the dissociation constants of aminium nitrate are greater than or equal to that of NH_4NO_3 (Murphy et al., 2007). Therefore, the formation of aminium salts by acid-base reactions in the presence of typical ambient ammonia levels is not favored. These results imply that other pathways contribute to the internal mixture of organic and inorganic aminium salts found in the atmosphere. It should be noted that ammonium salts are major components of atmospheric particles. If amines are taken up onto these pre-existing particles, they may form particulate organic amines. Thus, this heterogeneous reaction would explain the formation of internal mixture of organic and inorganic aminium salts. Very few studies have investigated the reactions between DMA, TMA, and clusters of NH_4HSO_4 and NH_4NO_3 (Bzdek et al., 2010a, b) between TMA and NH_4NO_3 particles (Lloyd et al., 2009), and between MA, DMA, and TMA and $(NH_4)_2SO_4$ and NH_4HSO_4 (Qiu et al., 2011). The uptake coefficient of TMA on NH_4NO_3 has been measured as $2 \pm 2 \times 10^{-3}$ (Lloyd et al., 2009), while the uptake coefficient for MA, DMA, and TMA by $(NH_4)_2SO_4$ has been measured as 2.6×10^{-2} to 3.4×10^{-2} (Qiu et al., 2011). The uptake coefficients of TMA and DMA on clusters (1-2 nm) of NH_4HSO_4 and NH_4NO_3 are close to unity (Bzdek et al., 2010a, b). The kinetics of these reactions in relation to the amine structure (Wang et al., 2010b) and also to the particle size of the ammonium salt (Bzdek et al., 2010a, b; Lloyd et al., 2009) have been discussed in few

studies. Recently, Chan and Chan (2012) also confirmed the displacement reaction between triethylamine (TEA) and $(NH_4)_2SO_4$, NH_4HSO_4, NH_4NO_3, NH_4Cl and $(NH_4)_2C_2O_4$ using *in situ* Raman spectroscopy. At present date, the reported uptake coefficients showed a discrepancy among different ammonium salts. However, it is hard to directly compare these results because of the difference in reaction conditions, such as the particle size, the type of amines and ammonium salts, and the reaction temperature used in experiments and so on. On the other hand, the relatively few kinetic data is available for one kind of amine. For example, as for MA, only one paper (Qiu et al., 2011) reported its uptake coefficient on $(NH_4)_2SO_4$. The uptake coefficients of MA on other salts are unknown. Thus, it is not clear yet that how the property of inorganic ammonium salts affects the reactivity for this reaction.

In this study, we investigated the heterogeneous uptake of MA on NH_4HSO_4, $(NH_4)_2SO_4$, NH_4NO_3 and NH_4Cl to understand the effect of ammonium salts on their reactivity with MA. We established for the first time the structure-reactivity relationship between MA and ammonium salts. The surface species during uptake were investigated using an *in situ* Raman spectrometer. The kinetic were measured at 298 K using a Knudsen cell reactor coupled to a quadrupole mass spectrometer (QMS). A linear free energy relationship was observed for the uptake of MA onto $(NH_4)_2SO_4$, NH_4NO_3 and NH_4Cl based on theoretical calculations. The environmental implications for these reactions were also discussed.

2. Experimental Details

2.1 Uptake experiments. We used a Knudsen cell reactor coupled to a QMS (KCMS, Hiden, HAL 3F PIC) to conduct the kinetic experiments (Liu et al., 2009a, b and 2010b, c). Briefly, the mass spectrometer was housed in a vacuum chamber equipped with a 300 $L \cdot s^{-1}$ turbomolecular pump (Pfeiffer) and an ion gauge (BOC Edward). The vacuum chamber between the QMS and the Knudsen cell reactor was pumped by a 60 $L \cdot s^{-1}$ turbomolecular pump for the mass spectrometer and ion gauge (both from BOC Edward) differential

100 pumping. The Knudsen cell reactor consisted of a stainless steel chamber with a gas inlet
101 controlled by a leak valve, an escape aperture whose area could be modified with an
102 adjustable iris, and a sample holder attached to the top ceiling of a circulating fluid bath. The
103 area of the escape aperture was set at 0.88 mm^2 during uptake experiments and measured
104 according to methods reported previously (Liu et al., 2009a, b and 2010a, b). The sample in
105 the sample holder was exposed to or isolated from the reactants by a lid connected to a linear
106 translator. The temperature of the sample holder was measured with an embedded Pt
107 resistance thermometer and held at 298 K ± 0.10 K using a super thermostat and cryofluid
108 pump (DFY-5/80, Henan Yuhua laboratory instrument Co, Ltd.).

109 Powder samples of ammonium salts were finely grounded and dispersed evenly on the
110 Teflon sample holder and then out-gassed at 298 K for 8 h to reach a base pressure of
111 approximately 5.0×10^{-7} Torr. After the sample cover was closed, MA gas equilibrated with
112 40 wt% methylamine solution was introduced into the reactor chamber through the leak valve.
113 The pressure in the reactor, which was controlled by the leak valve and measured using the
114 absolute pressure transducer, was $3.0 \pm 0.2 \times 10^{-5}$ Torr. Prior to the experiments, the reactor
115 chamber was passivated with amines for 90 min until a steady state QMS signal was
116 established as the samples were isolated from the gas by the sample cover. The observed
117 uptake coefficients (γ_{obs}) were calculated with a Knudsen cell equation (Tabor et al., 1994;
118 Ullerstam et al. 2003; Underwood et al., 2000).

119 $$\gamma_{obs} = \frac{A_h}{A_g} \cdot \frac{I_0 - I}{I} \quad (1)$$

120 Where, A_h is the effective area of the escape aperture (cm^2); A_g is the geometric area of the
121 sample holder (cm^2); and I_0 and I are the mass spectral intensities with the sample holder
122 closed and open, respectively.

123 Methylamine vapor was generated by 40 wt% of methylamine aqueous solution (Alfa
124 Aesar). Analytical grade ammonium salts including $(NH_4)_2SO_4$ (Beijing Chemical Regent),

125 NH_4HSO_4 (Beijing Zhongliante Chemical Co., Ltd.), NH_4NO_3 (Guangdong Xilong Chemical
126 Company) and NH_4Cl (Beijing Chemical Factory) were used after being finely grounded.
127 Their specific surface areas (N_2-BET) were measured around 0.1 $m^2 \cdot g^{-1}$ using a
128 Quantachrome Autosorb-1-C instrument.

129 **2.2 *In situ* Raman spectra measurements.** *In situ* Raman spectra for the reaction of
130 ammonium salts with MA were recorded on a UV resonance Raman spectrometer (UVR
131 DLPC-DL-03), which was described elsewhere (Liu et al., 2010a). The instrument was
132 calibrated against the Stokes Raman signal of Teflon at 1378 cm^{-1}. A continuous diode
133 pumped solid state (DPSS) laser beam (532 nm) was used as the exciting radiation, with the
134 adjustable source power ranging from 0 to 200 mW. A source power with 50 mW was used
135 and no sample modification was observed when the sample was irradiated under the
136 experimental conditions. The diameter of the laser spot on the sample surface was focused at
137 25 μm. The spectra resolution was 2.0 cm^{-1}. Ammonium salt powder was placed into a
138 stainless steel sample holder and purged with 100 mL/min of simulated air (80% high purity
139 N_2 and 20% high purity O_2) for 2 h at 298 K. Then, ca. 0.5 % of MA in 100 mL/min air was
140 carried by nitrogen from 40 % MA aqueous solution into the reactor and then *in situ* Raman
141 spectra were recorded. To avoid the influence of visible light on the heterogeneous reaction,
142 the sample was only exposed to the exciting laser for spectra collection. The exposure time
143 for each spectrum was 10 s with 6 scans. The temperature was held at 298 K during the
144 reaction.

145 **2.3 Computational methods**. We employ the Gaussian 09 suite of programs (Frisch et al.,
146 2009) to investigate the electrostatic potential of the ammonium salts. Geometry optimization
147 were performed within the premise of the density functional theory (DFT) using Becke's
148 three-parameter hybrid functional (B3) (Becke, 1993) combined with the electron-correlation

functional of Lee, Yang, and Parr (LYP) (Lee et al., 1988). 6-311++G (2df, 2p) basis set was used for all the calculations.

3. Results and discussion

3.1 Uptake of MA onto inorganic ammonium salts. Fig. 1 shows the typical mass spectra profiles for MA uptake onto $(NH_4)_2SO_4$, NH_4HSO_4, NH_4NO_3, and NH_4Cl at 298 K. According to the fragmentation patterns of CH_3NH_2, the fragment peak at *m/e*=30 (CH_2NH_2) had the strongest intensity, followed by the parent peak at *m/e*=31 (CH_3NH_2). Therefore, these two mass channels were scanned for MA measurement and shown in blue and red color, respectively. The mass channel of *m/e*=17 was monitored for the possible product of NH_3 and show in black color for the original signal and purple color for corrected one. The fragment peaks of H_2O (OH) and CH_3NH_2 (NH_3) may have also contributed to this mass channel. To determine the contribution of H_2O to *m/e*=17, the mass channels of *m/e*=18 (H_2O) shown in olive color was scanned because gaseous MA was generated using 40 wt% MA aqueous solution. For NH_4Cl samples, the mass channel of *m/e*=36 was additionally scanned for monitoring the decomposition of NH_4Cl.

Fig. 1

As shown in Figs. 1A and B, the signal change of MA (*m*/*e* = 30 and 31) was classified into three stages after the $(NH_4)_2SO_4$ sample was exposed to MA vapor. The first stage was the remarkable decrease in intensity with maximal amplitude of 67% within the first 2 min. The second was the quick recovery stage (from 2 min to 5 min) followed by the third stage with a slow recovery rate. Signal intensity recovered about 40% within 3 min of the second stage, and recovered a further 35% within 30 min of the third stage. As shown in Fig. 1, when the NH_4HSO_4, NH_4NO_3, and NH_4Cl samples were exposed to MA vapor, the signal intensity of MA (*m/e*=30 and *m/e*=31) only contained two stages. In the first stage, it decreased dramatically, followed by a gradual decrease to the lowest values with the maximal

amplitudes of 78 %, 75 % and 38%, respectively. In the second stage, the signal intensities of MA gradually increased with time and finally recovered about 10 %, 13%, and 33 % at 30 min, respectively. The signal recovery should be ascribed to desorption of MA or consumption of active sites over time. Because the experiments were conducted in a steady-state, the decrease in MA signal intensity indicated the loss of MA molecules from gas phase to the surface of these ammonium salt samples.

When the $(NH_4)_2SO_4$ sample was exposed to MA, the original profile for the *m/e*=17 mass channel (Fig. 1C) was, however, quite different from that of MA, though it also included the three stages, that is, a decrease, increase and then decrease in intensity. The complicated patterns of its signal profile implied that more than one species contributed to this mass channel. As mentioned above, H_2O, NH_3, and CH_3NH_2 may contribute to this mass channel. As shown in Fig. 1D, however, the signal intensity of *m/e*=18 remained almost unchanged when the sample was exposed to MA vapor. So it does (for *m/e*=18) when other samples were exposed to MA vapor (Figs. 1H, L, and P). Therefore, the contribution of H_2O to the *m/e*=17 mass channel was ignored because the intensity ratio of *m/e*=17 to that of *m/e*=18 was about 0.3 in pure water vapor (NIST). In Fig. 1C, the synchronous decrease in intensity of *m/e*=17, *m/e*=30, and *m/e*=31 in the first stage suggested that these three mass channels had the same source (CH_3NH_2). The same phenomenon was observed during the whole uptake stage for MA onto NH_4HSO_4 (Figs. 1E-G). It should be pointed out that the signal intensity of *m/e*=17 in Fig. 1C exceeded its baseline in the second stage (about 3 min after the sample cover was opened) and decreased slowly with time after reaching a maximal value (about 10 min). This implied a gaseous product (NH_3) also contributed to this mass channel during uptaking MA onto $(NH_4)_2SO_4$. As shown in Fig. 1G, a continuous decrease with an amplitude around 28 % for the signal intensity of *m/e*=17 was observed when the NH_4HSO_4 sample was exposed to MA vapor. Because the contribution of H_2O to this mass

channel was not important, the decrease of the signal intensity of *m/e*=17 can be mainly ascribed to consumption of MA. Figs. 1K and O show the evolution of the signal intensity of *m/e*=17 when NH_4NO_3 and NH_4Cl were exposed to MA vapor, respectively. Unlike those shown in Figs. 1C and G, significant increase in the intensity of *m/e*=17 occurred intermediately at the same time as NH_4NO_3 and NH_4Cl samples uptake MA. The purple curves for *m/e*=17 show the corrected signal originating from NH_3 after the contribution of MA to this mass channel was subtracted, using $\Delta I_{17}/\Delta I_{30}$=0.27 (Figs. 1E and G).

Fig. 2 shows the *In situ* Raman spectra for the heterogeneous reaction of MA with ammonium salts at 298 K. The insert graphs in purple box show the enlarged spectra in the range of 950-1080 cm^{-1} and those on the top right corner show the spectra in the range of 2500-3600 cm^{-1}. When the NH_4NO_3 sample was exposed to MA vapor, new bands at both 1008 cm^{-1} and 2981 cm^{-1} increased with time. The band at 1008 cm^{-1} was ascribed to the stretch vibration of C-N in MA and the band at 2981 cm^{-1} was related to that of CH_3 (Purnell et al., 1976). For $(NH_4)_2SO_4$ sample, the band at 2981 cm^{-1} was observed obviously while the band at 1008 cm^{-1} was observed as a shoulder peak because of the strong peak of SO_4^{2-} (ν_1) at 976 cm^{-1} (Kruus et al., 1985). It was inversed for NH_4Cl. The changes of other bands attributing to $(NH_4)_2SO_4$, NH_4NO_3 and NH_4Cl were unobservable. These results well supported the exchange reactions discussed above between MA and $(NH_4)_2SO_4$, NH_4NO_3 and NH_4Cl. However, when NH_4HSO_4 was exposed to MA vapor, the bands attributing to HSO_4^- at 1048, 1017, 884, 578, and 415 cm^{-1} (Kruus et al., 1985) decreased in intensity with time, accompanied with obvious increase of SO_4^{2-} (978 cm^{-1}), C-N (1008 cm^{-1}) and CH_3 (2986 cm^{-1}) in MA. The synchronous decrease in intensity of HSO_4^- with the increase of SO_4^{2-} suggested the transfer of H proton from HSO_4^- to MA, then leading to the formation of SO_4^{2-}. This result demonstrated that the active site for uptake of MA onto NH_4HSO_4 was the proton in HSO_4^-. These results were also well agreement with Knudsen cell experiments.

Fig. 2

Therefore, based on these results, we concluded that except for NH_4HSO_4, exchange reaction between CH_3NH_2 and $(NH_4)_2SO_4$, NH_4NO_3 and NH_4Cl occurred under these conditions. As for NH_4HSO_4, a simple acid-base reaction occurred and the proton in HSO_4^- should be the reactive site. These reactions can be summarized as follows.

$$CH_3NH_2 + (NH_4)_2SO_4 \rightarrow CH_3NH_3(NH_4)SO_4 + NH_3 \quad (2)$$

$$CH_3NH_2 + CH_3NH_3(NH_4)SO_4 \rightarrow (CH_3NH_3)_2SO_4 + NH_3 \quad (3)$$

$$CH_3NH_2 + NH_4HSO_4 \rightarrow CH_3NH_3(NH_4)SO_4 \quad (4)$$

$$CH_3NH_2 + NH_4NO_3 \rightarrow CH_3NH_3NO_3 + NH_3 \quad (5)$$

$$CH_3NH_2 + NH_4Cl \rightarrow CH_3NH_3Cl + NH_3 \quad (6)$$

Because one $(NH_4)_2SO_4$ molecule contains two NH_4^+ ions, the exchange reaction between MA and $(NH_4)_2SO_4$ may involve two steps. Similar exchange reactions have been observed in previous studies between DMA, TMA, and clusters of NH_4HSO_4 and NH_4NO_3 (Bzdek et al., 2010a, b), between TMA and NH_4NO_3 particles (Lloyd et al., 2009), and between MA, DMA, TMA and $(NH_4)_2SO_4$ and NH_4HSO_4 (Qiu et al., 2011).

3.2 Stability of aminium salts. To investigate the stability of aminium salts formed on the surface, desorption experiments were performed after the completion of the uptake experiments. After the sample was isolated from the feed gas by the sample cover, the introduction of feed gas into the reactor was stopped. When a steady-state mass spectrometry signal was established, the sample cover was opened and the desorbed species were monitored online with the QMS. The escape aperture area was increased to 5.5 mm^2 from 0.88 mm^2 in some cases using the variable iris to increase the gas flow rate from the Knudsen cell reactor into the QMS detector. The mass channels were scanned as the same as that during uptake experiments. Figs. 3A-D show the mass spectra of the cared desorbates from

248 58.2 mg $(NH_4)_2SO_4$, 60.5 mg NH_4HSO_4, 59.8 mg NH_4NO_3, 63.9 mg NH_4Cl, respectively,
249 after exposed to MA for ca. 30 min.

250 As shown in Figs. 3A and B, no desorption of MA and NH_3 was observed at 298 K from
251 MA treated $(NH_4)_2SO_4$ and NH_4HSO_4 samples even though a maximal A_h (5.5 mm^2) was
252 used. This indicated that the uptake of MA onto the surface of $(NH_4)_2SO_4$ and NH_4HSO_4 is
253 irreversible and $CH_3NH_3(NH_4)SO_4$ and $(CH_3NH_3)_2SO_4$ are stable under these conditions.
254 This was similar to the irreversible exchange reactions between DMA or TMA and
255 ammonium bisulfate clusters reported by Bzdek et al. (2010a).

256 Fig. 3

257 As shown in Fig. 3C and D, when the sample cover was opened with the same A_h used
258 in the uptake experiments (0.88 mm^2), desorption of CH_2NH_2 and CH_3NH_2 from the MA
259 exchanged NH_4NO_3 and NH_4Cl sample was very weak, while release of NH_3 (Figs. 3C and D)
260 was very clear. To increase the signal of the mass spectrometer, maximal A_h was used
261 through adjusting the iris. The signal intensities of the *m/e*=30 and *m/e*=17 mass channels
262 increased obviously and were accompanied by a faint increase in the mass channel of *m/e*=31
263 when the sample cover was opened. In Fig3 C, both CH_2NH_2 and NO contributed to the
264 *m/e*=30 mass channel, while the signal change of *m/e*=31 only resulted from CH_3NH_2.
265 According to the $\Delta I_{31}/\Delta I_{30}$ = 0.60 calculated in Fig. 1 and the signal intensity in Fig. 3C, the
266 fragment ion of MA (CH_2NH_2) was estimated contributing 15% to the signal change of the
267 *m/e*=30 in Fig. 3C.

268 It should be noted that NH_4NO_3 easily decomposes into NH_3 and HNO_3 under low
269 pressure conditions (Lightstone et al., 2000). Other ammonium salts might also undergo
270 decomposition reaction. Therefore, the decomposition experiments for pure ammonium salts
271 were performed under the similar conditions. The mass spectra for pure $(NH_4)_2SO_4$ and
272 NH_4HSO_4 when evacuated at 1.2 $\times 10^{-6}$ Torr and at 298 K (not shown) were the same as those

shown in Figs. 3A and B, which suggested that decomposition of $(NH_4)_2SO_4$ and NH_4HSO_4 are negligible under these conditions. Fig. 3E shows the mass spectra of desorbates from pure NH_4NO_3. Observable decomposition of NH_4NO_3 occurred under these conditions. In Fig 3E, the $\Delta I_{17(NH3)}/\Delta I_{30(NO)}$ could be normalized to 1 because the mass channels of *m/e*=30 and *m/e*=17 were the result of the dissociation of NH_4NO_3. The normalized ratio of $\Delta I_{17(NH3)}/\Delta I_{30(NO+CH2NH2)}$ was 0.85. This also meant that desorption of MA (CH_2NH_2) explained 15% of the *m/e*=30 signal change in Fig. 3C. Therefore, the increase in *m/e*=30 signal intensities (Fig. 3C) were mainly from the decomposition of the unreacted NH_4NO_3. Fig. 3F shows the desorption of NH_3 and HCl (*m/e*=36, 3 times of magnification) from pure NH_4Cl. It was almost unobservable for desorption of NH_3 and HCl with the A_h of 0.88 mm^2; while a weak desorption of NH_3 and HCl can be discerned when the A_h was increased to 5.5 mm^2. It meant that dissociation of both NH_4Cl and CH_3NH_3Cl should contribute to the signals in Fig. 3D. According to the value of $I_{17}/\Delta I_{30}$=0.27 and the change of signal intensity of *m/e*=30 in Fig. 3D, we estimated that decomposition of CH_3NH_3Cl contributes 12 % to the intensity change of the *m/e*=30 in Fig. 3D. Thus, we can conclude that $CH_3NH_3NO_3$ and CH_3NH_3Cl are not stable at low pressure and they have higher dissociation vapor pressure than methylammonium sulfate.

3.3 Kinetics of MA uptake onto ammonium salts. As discussed above, the signal intensities of *m/e*=30 and *m/e*=31 decreased synchronously when the sample cover was opened. Because the signal intensity of *m/e*=30 was linearly correlated with that of *m/e*=31 (I_{31} = 0.60I_{30}, R = 0.997), either can be used to calculate the γ_{obs} according to Eq. 1. As discussed above, decomposition of NH_4NO_3 can contribute to the mass channel of *m/e*=30. However, when the signal change in Fig. 2E was compared to that in Fig. 1I, the compensation effect of NH_4NO_3 decomposition to the signal intensity of *m/e*=30 is

297 neglectable. Thus, in the following section, the signal intensity of *m/e*=30 was used for
298 uptake coefficient calculations.

299 Fig. 4

300 Fig. 4 illustrate typical profiles of the observed uptake coefficient as a function of time
301 at 298 K. The γ_{obs} of MA on $(NH_4)_2SO_4$ decreased with exposure time (Fig. 3A)
302 corresponding to the recovery of the MA signal (Fig. 1A). In Fig. 4, the γ_{obs} of MA on
303 NH_4HSO_4, NH_4NO_3, and NH_4Cl also showed a slow decline with time after the maximal
304 value was reached. As discussed above, neither desorption of MA nor the dissociation of
305 aminium salts formed on the $(NH_4)_2SO_4$ and NH_4HSO_4 surface occurred; therefore, the
306 decrease in the uptake coefficient of MA on $(NH_4)_2SO_4$ and NH_4HSO_4 was ascribed to the
307 depletion of active sites over time. As for NH_4NO_3 and NH_4Cl, although the exchange
308 reactions were partially reversible, the dissociation rates of $CH_3NH_3NO_3$ and CH_3NH_3Cl
309 were slower than their formation rates. Therefore, accessible active sites also decreased with
310 time. Table 1 summaries the initial uptake coefficients of MA onto $(NH_4)_2SO_4$, NH_4HSO_4,
311 NH_4NO_3 and NH_4Cl at 298 K.

312 Previous research has found that γ_{obs} depends on sample mass due to the diffusion of
313 reactant gas into the underlying layers of the multilayer powder sample (Liu et al., 2009a,b
314 and 2010b,c; Ullerstam et al., 2003; Underwood et al., 2000 and 2001). Some studies have
315 found, however, that uptake coefficient is unrelated to sample mass (Qiu et al., 2011; Seisel
316 et al., 2005). In the present work, we performed uptake experiments on a wide range of
317 sample masses. When the sample mass was lower than 40.0 mg, it was difficult to cover the
318 sample holder with salt particles evenly. Therefore, uptake experiments on samples with
319 masses lower than 40 mg were not performed. Sample mass dependence was not observed for
320 the γ_{obs} of MA on all of these salts. This indicates that the underlayers of the sample
321 contributed very little to MA uptake. This phenomenon also supported the slight declines of

uptake coefficient with exposure time (Fig. 4) because the reactions were confined on the surface. The same phenomena was also observed for the uptake of MA, DMA, and TMA on $(NH_4)_2SO_4$ (Qiu et al., 2011). On the other hand, when the QMS signal intensity (*I*) was calibrated with molecular flow rate ($mol \cdot s^{-1}$) (Liu et al., 2008), the amount of MA uptake onto ammonium salts can be calculated using the integrated area shown in Fig. 1. They are 6.0×10^{-7}, 1.1×10^{-6}, 1.2×10^{-6}, and 3.9×10^{-7} moles on $(NH_4)_2SO_4$, NH_4HSO_4, NH_4NO_3, and NH_4Cl, respectively. The amount of ammonium salts are 4.4×10^{-4}, 5.3×10^{-4}, 7.5×10^{-4} and 1.2×10^{-3} moles, respectively. Therefore, the ratio between uptaked amine and ammonium salts during the reaction are estimated to be 0.14 %, 0.21 %, 0.16 % and 0.03 % on $(NH_4)_2SO_4$, NH_4HSO_4, NH_4NO_3, and NH_4Cl, respectively. If two ammonium ions in $(NH_4)_2SO_4$ involve in the exchange reaction, the ratio should be 0.07 %. It means than only a very small fraction of ammonium salts, most probably confined on the surface, involves in this heterogeneous reaction. Therefore, it was reasonable to speculate that the true uptake coefficient (γ_t) was very close or equal to the γ_{obs}. As shown in Table 1, the average γ_{obs} of MA on $(NH_4)_2SO_4$, NH_4HSO_4, NH_4NO_3 and NH_4Cl at 298 K was $6.30 \pm 1.03 \times 10^{-3}$, $1.78 \pm 0.36 \times10^{-2}$, $8.79 \pm 1.99 \times 10^{-3}$ and $2.29 \pm 0.28 \times 10^{-3}$, respectively. The uptake coefficients of MA onto $(NH_4)_2SO_4$, NH_4Cl and NH_4NO_3 measured in this work are comparable to that of TMA on NH_4NO_3 ($2 \pm 2 \times 10^{-3}$) reported by Lloyd et al. (2009), while they are two orders of magnitude lower than the values for DMA and TMA uptake on clusters of NH_4HSO_4 and NH_4NO_3 reported by Bzdek et al. (2010a, b). The uptake coefficient of MA onto NH_4HSO_4 is comparable to that on sulfuric acid (Wang et al., 2010a). As for the uptake of MA on $(NH_4)_2SO_4$, uptake coefficients were slightly lower than the value (2.6×10^{-2} - 3.4×10^{-2}) reported by Qiu et al. (2011). Recently, Chan and Chan (2012) found that amorphous NH_4NO_3 and NH_4HSO_4 showed higher degree of exchange reaction to TEA than that of crystalline NH_4NO_3 and NH_4HSO_4. Thus, the difference in the uptake coefficient may be

ascribed to different reaction systems, different samples with different particle sizes or morphology. In the studies by Bzdek et al (2010a, b), for example, 1-2 nm clusters of bisulfate or nitrate were used, and amorphous $(NH_4)_2SO_4$ was used by Qiu et al. (2011); while crystal samples were used in the present study. In ambient environments, however, low RH conditions may also induce potential crystallization of these ammonium salts (Clegg et al., 1998). Thus, the uptake coefficients reported here should represent the low limits for uptake of MA on ammonium salts.

Table 1

3.4 Effect of property of ammonium salts on the heterogeneous reaction. Above results demonstrated that exchange reaction between MA and $(NH_4)_2SO_4$, NH_4NO_3 and NH_4Cl occurred, while only acid-base reaction took place on NH_4HSO_4. In general speaking, these reactions can be regarded as electrophilic reaction, in which the lone-pair electron in CH_3NH_2 was the active center. The molecular electrostatic potential (MEP) is widely used as a reactivity map displaying most probable regions for the electrophilic attack of charged point-like reagents (Politzer et al., 1981). In the reactions of a series of related molecules, A_1, A_2, …, A_n, with some given reactant B, the differences in the activation energies are linearly related to the differences in the heats of reaction, namely, a linear free energy relationship. Because electrostatic potential can be used as a measurement of thermodynamic, the electrostatic potentials at some particular sites in such a series of molecules are related to their interaction energies with B. Therefore, MEP is also used to correlate with the reaction mechanism and kinetics (Politzer et al., 1985).

Fig. 5 shows the MEP of ammonium salts calculated at B3LYP/6-311++G (2df, 2p) level. The geometries for these salts were also optimized at the same level and the true minimal was confirmed without imaginary frequency. As shown in Fig. 5, the maximal value for electrostatic potential located at the H atom in the NH_4^+ group and were 827.58, 1386.38,

372 1741.85, and 637.42 kJ/mol for NH_4Cl, $(NH_4)_2SO_4$, NH_4NO_3, and NH_4HSO_4, respectively.
373 Fig. 6 indicates the correlation between the lnγ of MA onto these ammonium salts with the
374 corresponding MEP. As can be seen in Fig. 6, a linear correlation between the lnγ and MEP
375 were observed among NH_4Cl, $(NH_4)_2SO_4$, and NH_4NO_3, with a high correlation coefficient
376 (R=0.991). NH_4NO_3 with the highest MEP had the largest uptake coefficient. However,
377 NH_4HSO_4 obviously deviated this linear relationship. This deviation can be ascribed to the
378 different reaction mechanism as discussed above. This result also implied that the first step
379 for the heterogeneous reactions between MA and NH_4Cl, $(NH_4)_2SO_4$, and NH_4NO_3 should be
380 adsorption of MA onto the NH_4^+ group, in which H atom should be the active site.
381 Fig. 5
382 Fig. 6
383 **4. Conclusions and atmospheric implications.**
384 In this work, the heterogeneous reactions of MA on the typical ammonium salts
385 including $(NH_4)_2SO_4$, NH_4HSO_4, NH_4NO_3 and NH_4Cl were investigated by using Knudsen
386 cell reactor, Raman spectroscopy and theoretical calculations. Exchange reactions between
387 MA and $(NH_4)_2SO_4$, NH_4NO_3 and NH_4Cl were observed, while acid-base reaction was found
388 between MA and NH_4HSO_4. The stability of $CH_3NH_3NH_4SO_4$ or $(CH_3NH_3)_2SO_4$ were found
389 to be stronger than $CH_3NH_3NO_3$ and CH_3NH_3Cl under low pressure. The observed uptake
390 coefficients of MA on these salts can be used as the true uptake coefficients because diffusion
391 of MA into the underlayers of powder samples was neglectable. The uptake coefficients were
392 $6.30 \pm 1.03 \times 10^{-3}$, $1.78 \pm 0.36 \times 10^{-2}$, $8.79 \pm 1.99 \times 10^{-3}$ and $2.29 \pm 0.28 \times 10^{-3}$ on $(NH_4)_2SO_4$,
393 NH_4HSO_4, NH_4NO_3 and NH_4Cl at 298 K, respectively. As for $(NH_4)_2SO_4$, NH_4Cl, and
394 NH_4NO_3, the structure-reactivity relationship was established, namely, natural logarithm of
395 the uptake coefficients were highly linear related with the MEP of the H atom in the NH_4^+

group. It means property of ammonium salts have strong influence on the reactivity of MA with these ammonium salts.

Field measurements have found that aminium salts are usually internally mixed with inorganic ammonium salts in atmospheric particulate matter (Facchini et al., 2008; Pratt et al., 2009; Smith et al., 2010). In general, acid-base reactions between amines and H_2SO_4 or HNO_3 are considered the main source of particulate aminium salts. For example, Wang et al. (2010a) measured the uptake coefficients of MA on 62-82 wt% of H_2SO_4 to be $2.0 \pm 0.2 \times 10^{-2}$ to $3.2 \pm 0.5 \times 10^{-2}$ at 283 K. This is four to ten times higher than the γ_{obs} for MA on NH_4NO_3, $(NH_4)_2SO_4$ or NH_4Cl, while it is comparable to the uptake coefficient of MA onto NH_4HSO_4 measured in this work. When the abundance of ammonium salts in the troposphere as well as the relatively large uptake coefficients of MA on them are considered, uptake of MA onto ammonium salts should not be ignored. Of course, it should be pointed out that our experiments were carried out under dry condition and the clean surface of ammonium salts was studied. In the real atmosphere, high relative humidity (RH) and organic species on the surface might have complex influence on this reaction. Recently, Chan and Chan (2012) found that aqueous salts of $(NH_4)_2SO_4$, NH_4HSO_4 and NH_4Cl show higher degree of exchange reaction to TEA. It implies the uptake coefficients of MA on these salts might also be larger under ambient RH than these measured under dry conditions. In ambient environments, however, low RH conditions may also induce potential crystallization of these ammonium salts (Clegg et al., 1998). Thus, as the low limits for uptake coefficient of MA onto ammonium salts, the measurements in this study at least suggest that amines uptake onto pre-existing ammonium salts even under dry conditions may contribute, under particular circumstances, as high concentrations of ammonium salts and low concentration of acidic gas species, to the atmospheric source of particulate amines.

Acknowledgements

This research was funded by the National Natural Science Foundation of China (50921064, 20937004 and 20907069).

References

Becke, A. D. Density-functional thermochemistry. III. The role of exact exchange. *J. Chem. Phys*., 98, 5648-5652, **1993**.

Beddows, D. C. S.; Donovan, R. J.; Harrison, R. M.; Heal, M. R.; Kinnersley, R. P.; King, M. D.; Nicholson, D. H.; Thompson, K. C., Correlations in the chemical composition of rural background atmospheric aerosol in the UK determined in real time using time-of-flight mass spectrometry *J. Environ. Monit.*, 6, 124-133, **2004**.

Bzdek, B. R.; Ridge, D. P.; Johnston, M. V., Amine exchange into ammonium bisulfate and ammonium nitrate nuclei. *Atmos. Chem. Phys.*, 10, 3495-3503, **2010a**.

Bzdek, B. R.; Ridge, D. P.; Johnston, M. V., Size-dependent reactions of ammonium bisulfate clusters with dimethylamine. *J. Phys. Chem. A*, *114*,11638-11644, **2010b**.

Chan, L.P.; Chan, C.K. Displacement of ammonium from aerosol particles by uptake of triethylamine. *Aerosol Sci. Technol*., 46, 236-247, **2012**.

Chen, H.; Chen, L.; Chiang, Z.; Hung, C.; Lin, F.; Chou, W.; Gong, G.; Wen, L., Size fractionation and molecular composition of water-soluble inorganic and organic nitrogen in aerosols of a coastal environment. *J. Geophy. Res.*, *115(D22307)*, 10.1029/2010jd014157, **2010**.

Clegg, S. L.; Brimblecombe, P.; Wexler, A. S. Thermodynamic model of the system H^+–NH_4^+–SO_4^{2}–NO_3–H_2O at tropospheric temperatures. *J. Phys. Chem. A*, 102, 2137–2154, **1998**.

444 Cornell, S. E.; Jickells, T. D.; Cape, J. N.; Rowland, A. P.; Duce, R. A., Organic nitrogen
445 deposition on land and coastal environments: a review of methods and data. *Atmos. Environ.*,
446 37, 2173-2191, **2003**.
447 Facchini, M. C.; Decesari, S.; Rinaldi, M.; Carbone, C.; Finessi, E.; Mircea, M.; Fuzzi, S.;
448 Moretti, F.; Tagliavini, E.; Ceburnis, D.; O'Dowd, C. D., Important source of marine
449 secondary organic aerosol from biogenic amines. *Environ. Sci. Technol.*, 42, 9116-9121,
450 **2008**.
451 Frisch, M. J.; Trucks, G. W.; Schlegel, H. B.; Scuseria, G. E.; Robb, M. A.; Cheeseman, J. R.
452 G.; Calmani, V.; Barone, B.; Mennucci, G. A.; Petersson, H.; Nakatsuji, M.; Caricato, Li, X.;
453 Hratchian, H. P.; Izmaylov, A. F.; Bloino, J.; Zheng, G.; Sonnenberg, J. L.; Hada, M.; Ehara,
454 M.; Toyota, K.; Fukuda, R.; Hasegawa, J.; Ishida, M.; Nakajima, T.; Honda, Y.; Kitao, O.;
455 Nakai, H.; Vreven, T.; Montgomery, J. A.; Peralta, J. E. F., Jr.; Ogliaro, M.; Bearpark, J. J.;
456 Heyd, E.; Brothers, K. N.; Kudin, V. N.; Staroverov, R.; Kobayashi, J.; Normand, K.;
457 Raghavachari, A.; Rendell, J. C.; Burant, S. S.; Iyengar, J.; Tomasi, M.; Cossi, N.; Rega, J.
458 M.; Millam, M.; Klene, J. E.; Knox, J. B.; Cross, V.; Bakken, C.; Adamo, J.; Jaramillo,
459 R.;Gomperts, R. E.; Stratmann, O.; Yazyev, A. J.; Austin, R.; Cammi, C.; Pomelli, J. W.;
460 Ochterski, R. L.; Martin, K.; Morokuma, V. G.; Zakrzewski, G. A.; Voth, P.; Salvador, J. J.;
461 Dannenberg, S.; Dapprich, A. D.; Daniels, O.; Farkas, J. B.; Foresman, J. V.; Ortiz, J.;
462 Cioslowski Fox, D. J. Gaussian 09; Gaussian, Inc.: Wallingford, CT, **2009**.
463 Gai, Y.; Ge, M.; Wang, W., Rate constants for the gas phase reactions of ozone with
464 diethylamine and triethylamine. *Acta Phys.-Chim. Sin.*, 26, 1768-1772, **2010**.
465 Ge, X.; Wexler, A. S.; Clegg, S. L., Atmospheric amines - Part II. Thermodynamic properties
466 and gas/particle partitioning. *Atmos. Environ.*, 45, 561-577**, 2011a**.
467 Ge, X.; Wexler, A. S.; Clegg, S. L., Atmospheric amines - Part I. A review. *Atmos. Environ.*,
468 45, 524-546, **2011b**.

469 Gong, W. L.; Sears, K. J.; Alleman, J. E.; Blatchley, E. R., Toxicity of model aliphatic
470 amines and their chlorinated forms. *Environ. Toxicol. Chem.*, *23*, 239-244, **2004**.
471 Kruus, P.; Hayes, C. A.; Adams, W. A. Determination of ratios of sulfate to bisulfate ions in
472 aqueous solutions by Raman spectroscopy. *J. Solution Chem.*, 14, 117-128, **1985**.
473 Lee, C.; Yang, W.; Parr, R. G. Development of the Colle-Salvetti correlation-energy formula
474 into a functional of the electron density. *Phys. Rev. B*, 37, 785-789, **1988**.
475 Liggio, J.; Li, S.-M.; Vlasenko, A.; Stroud, C.; Makar, P., Depression of ammonia uptake to
476 sulfuric acid aerosols by competing uptake of ambient organic gases. *Environ. Sci. Technol.*,
477 45, 2790-2796, **2011**.
478 Lightstone, J. M.; Onasch, T. B.; Imre, D. O., S., Deliquescence, efflorescence, and water
479 activity in ammonium nitrate and mixed ammonium nitrate/succinic acid microparticles. *J.*
480 *Phys. Chem. A,* 104, 9337-9346, **2000**.
481 Liu, Y. C.; He, H.; Mu, Y. J., Heterogeneous reactivity of carbonyl sulfide on α-Al_2O_3 and
482 γ-Al_2O_3. *Atmos. Environ.*, 42, 960-969, **2008**.
483 Liu, Y. C.; He, H., Experimental and theoretical study of hydrogen thiocarbonate for
484 heterogeneous reaction of carbonyl sulfide on magnesium oxide. *J. Phys. Chem. A*, *113*,
485 3387-3394, **2009a**.
486 Liu, Y. C., Liu, C., Ma, J. Z., Ma, Q. X., He, H., Structural and hygroscopic changes of soot
487 during heterogeneous reaction with O_3. *Phys. Chem. Chem. Phys.*, 12, 10896-10903, **2010a**.
488 Liu, Y.; Ma, J.; He, H., Heterogeneous reactions of carbonyl sulfide on mineral oxides:
489 mechanism and kinetics study. *Atmos. Chem. Phys.*, 10, 10335-10344, **2010b**.
490 Liu, Y. C.; Ma, J. Z.; Liu, C.; He, H., Heterogeneous uptake of carbonyl sulfide onto
491 kaolinite within a temperature range of 220–330 K. *J. Geogorphy. Res.*, 115(D24311),
492 doi:10.1029/2010JD014778, **2010c**.

493 Liu, Y. ; Ma, Q. ; He, H., Comparative study of the effect of water on the heterogeneous
494 reactions of carbonyl sulfide on the surface of α-Al_2O_3 and MgO. *Atmos. Chem. Phys.*, 9,
495 6273-6286, **2009b**.
496 Lloyd, J. A.; Heaton, K. J.; Johnston, M. V., Reactive uptake of trimethylamine into
497 ammonium nitrate particles. *J. Phys. Chem. A*, 113, 4840-4843, **2009**.
498 Murphy, S. M.; Sorooshian, A.; Kroll, J. H.; Ng, N. L.; Chhabra, P.; Tong, C.; Surratt, J. D.;
499 Knipping, E.; Flagan, R. C.; Seinfeld, J. H., Secondary aerosol formation from atmospheric
500 reactions of aliphatic amines. *Atmos. Chem. Phys.,* 7, 2313-2337, **2007**.
501 Politzer, P.; Truhlar, D.G. (Eds.), Chemical application of atomic and molecular electrostatic
502 potentials, Plenum, New York, **1981**.
503 Politzer, P.; Laurence, P. R.; Jayasuriya, K. Molecular electrostatic potentials: An effective
504 tool for the elucidation of biochemical phenomena. *Environ. Health Persp*., 61, 191-202,
505 **1985**.
506 Pratt, K. A.; Hatch, L. E.; Prather, K. A., Seasonal volatility dependence of ambient particle
507 phase amines. *Environ. Sci. Technol.*, 43, 5276-5281, **2009**.
508 Purnell, C. J.; Barnes, A. J.; Suzuki, S.; Ball, D.F.; Orville-Thomas, W.J.. Infrared and
509 Raman matrix isolation studies of methylamine. *Chem. Phys*., 12, 77-87, **1976**.
510 Qiu, C.; Wang, L.; Lal, V.; Khalizov, A. F.; Zhang, R., Heterogeneous reactions of
511 alkylamines with ammonium sulfate and ammonium bisulfate. *Environ. Sci Technol.*, 45,
512 4748-4755, **2011**.
513 Seisel, S.; Börensen, C.; Vogt, R.; Zellner, R., Kinetics and mechanism of the uptake of N_2O_5
514 on mineral dust at 298K. *Atmos. Chem. Phys.*, 5, 3423-3432, **2005**.
515 Shi, Q.; Davidovits, P.; Jayne, J. T.; Worsnop, D. R.; Kolb, C. E., Uptake of gas-phase
516 ammonia. 1. Uptake by aqueous surfaces as a function of pH. *J. Phys. Chem. A*, 103,
517 8812-8823, **1999**.

518 Silva, P. J.; Erupe, M. E.; Price, D.; Elias, J.; G. J. Malloy, Q.; Li, Q.; Warren, B.; Cocker, D.
519 R., Trimethylamine as precursor to secondary organic aerosol formation via nitrate radical
520 reaction in the atmosphere. *Environ. Sci. Technol.*, 42, 4689-4696, **2008**.
521 Smith, J. N.; Barsanti, K. C.; Friedli, H. R.; Ehn, M.; Kulmala, M.; Collins, D. R.;
522 H.Scheckman, J.; Williams, B. J.; McMurry, P. H., Observations of aminium salts in
523 atmospheric nanoparticles and possible climatic implications. *Proceed. Nat. Acad. Sci.*, 107,
524 6634-6639, **2010**.
525 Swartz, E.; Shi, Q.; Davidovits, P.; Jayne, J. T.; Worsnop, D. R.; Kolb, C. E., Uptake of
526 gas-phase ammonia. 2. Uptake by sulfuric acid surfaces. *J. Phys. Chem. A*, 103, 8824-8833,
527 **1999**.
528 Tabor, K.; Gutzwiller, L.; Rossi, M. J., Heterogeneous chemical kinetics of NO_2 on
529 amorphous carbon at ambient temperature. *J. Phys. Chem. A*, *98,* 6172-6186, **1994**.
530 Underwood, G. M.; Li, P.; Al-Abadleh, H. A.; Grassian, V. H., A Knudsen cell study of the
531 heterogeneous reactivity of nitric acid on oxide and mineral dust particles. *J. Phys. Chem. A,*
532 105, 6609-6620, **2001**.
533 Underwood, G. M.; Li, P.; Usher, C. R.; Grassian, V. H., Determining accurate kinetic
534 parameters of potentially important heterogeneous atmospheric reaction on solid particle with
535 a Knudsen cell reactor. *J. Phys. Chem. A*, *104,* 819-829, **2000**.
536 Ullerstam, M.; Johnson, M. S.; Vogt, R.; Ljungström, E., DRIFTS and Knudsen cell study of
537 the heterogeneous reactivity of SO_2 and NO_2 on mineral dust. *Atmos. Chem. Phys.*, 3
538 2043-2051, **2003**.
539 Wang, L.; Khalizov, A.F.; Zheng, J.; Xu, W.; Ma, Y.; Lal, V.; Zhang, R.Y.; Atmospheric
540 nanoparticles formed from heterogeneous reactions of organics. *Nat. Geosci.*, 3, 238-242,
541 **2010a**.

542 Wang, L.; Lal, V.; Khalizov, A. F.; Zhang, R., Heterogeneous chemistry of alkylamines with
543 sulfuric acid: Implications for atmospheric formation of alkylaminium sulfates. *Environ. Sci.*
544 *Technol.*, 44, 2461-2465, **2010b**.
545 Wang, X. F.; Gao, S.; Yang, X.; Chen, H.; Chen, J. M.; Zhuang, G. S.; Surratt, J. D.; Chan,
546 M. N.; Seinfeld, J. H., Evidence for high molecular weight nitrogen-containing organic salts
547 in urban aerosols. *Environ. Sci. Technol.*, *44*, 4441-4446, **2010c**.
548
549
550
551
552
553
554
555
556
557
558
559
560
561
562
563
564
565
566

Figure Legends

Fig. 1. Mass spectra profiles for uptake of MA onto (A-D) 58.2 mg of $(NH_4)_2SO_4$, (E-H) 60.5 mg NH_4HSO_4, (I-L) 59.8 mg NH_4NO_3, and (M-P) 63.9 mg NH_4Cl at 298 K. The blue curves are for *m/e*=30; the red curves are for *m/e*=31; the black and purple curves are for *m/e*=17; and the olive curves are for *m/e*=18.

Fig. 2 *In situ* Raman spectra for heterogeneous reactions of MA with ammonium salts at 298 K. The insert graphs in purple boxes show the enlarged spectra in the range of 950-1080 cm^{-1} and those on the top right corner show the spectra in the range of 2500-3600 cm^{-1}.

Figure 3. Desorption of surface species from MA treated salts and pure salts at 1.2 $\times 10^{-6}$ Torr and at 298 K. (A) 58.2 mg $(NH_4)_2SO_4$, (B) 60.5 mg NH_4HSO_4, (C) 59.8 mg NH_4NO_3, (D) 63.9 mg NH_4Cl, (E) 59.8 mg pure NH_4NO_3 and (F) 60.5 mg pure NH_4Cl. The A_h is 0.88 mm^2 in left side of the dash lines, and it is 5.5 mm^2 in the right side of the dash lines.

Fig. 4. Typical observed uptake coefficients of MA onto ammonium salts at 298 K.

Fig. 5. Electrostatic potential maps for ammonium salts.

Fig. 6. Relationship between uptake coefficients of MA onto ammonium salts and the electrostatic potential of H atom in NH_4^+.

592 Table 1. Uptake coefficients of MA onto ammonium salts at 298 K

$(NH_4)_2SO_4$		NH_4HSO_4		NH_4NO_3		NH_4Cl	
Sample mass (mg)	γ_{ini}	Sample mass(mg)	γ_{ini}	Sample mass(mg)	γ_{ini}	Sample mass (mg)	γ_{ini}
39.8	7.70E-03	40.4	1.60E-02	40.3	8.16E-03	63.9	2.35E-03
41.1	5.19E-03	39.8	1.90E-02	40.1	5.56E-03	66.1	2.46E-03
50.8	5.26E-03	60.5	1.82E-02	59.8	7.76E-03	81.1	2.35E-03
50.9	8.01E-03	61.5	1.91E-02	59.8	9.37E-03	81.9	1.89E-03
58.2	6.45E-03	85.0	1.90E-02	80.1	1.01E-02	101.7	2.72E-03
60.4	6.99E-03	83.8	1.37E-02	80.7	1.01E-02	103.7	2.01E-03
80.8	6.58E-03	103.2	1.33E-02	100.5	8.78E-03	121.7	2.46E-03
79.9	4.82E-03	102.5	2.33E-02	101.0	6.79E-03	124.2	2.09E-03
100.6	5.53E-03	123.7	1.35E-02	120.4	1.32E-02	-	-
101.0	6.43E-03	124.0	2.24E-02	121.0	8.07E-03	-	-
Average	6.30±1.08E-3	Average	1.78±0.36E-2	Average	8.79±2.10E-3	Average	2.29±0.28E-3

593

594

595

596

597

598

599

600

601

602

603

604

605

606

607

608

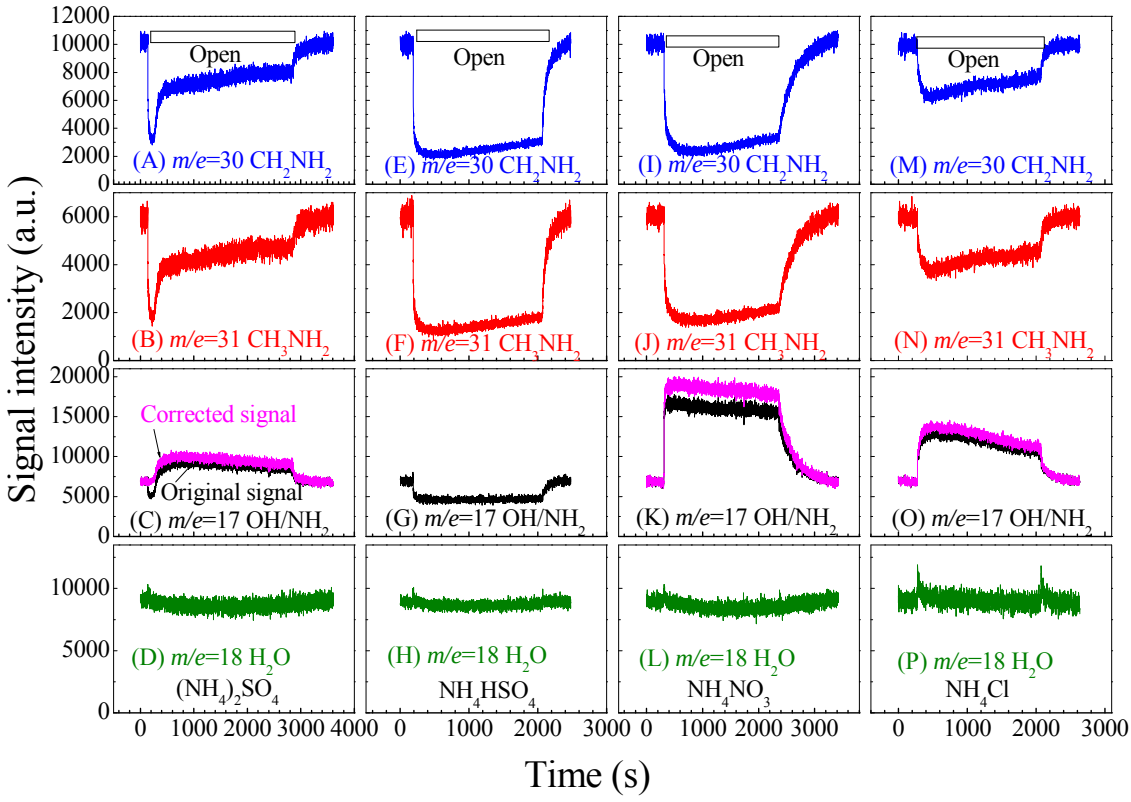

609

610 Fig. 1. Mass spectra profiles for uptake of MA onto (A-D) 58.2 mg of $(NH_4)_2SO_4$, (E-H) 60.5

611 mg NH_4HSO_4, (I-L) 59.8 mg NH_4NO_3, and (M-P) 63.9 mg NH_4Cl at 298 K. The blue curves

612 are for *m/e*=30; the red curves are for *m/e*=31; the black and purple curves are for *m/e*=17;

613 and the olive curves are for *m/e*=18.

614

615

616

617

618

619

620

621

622

623

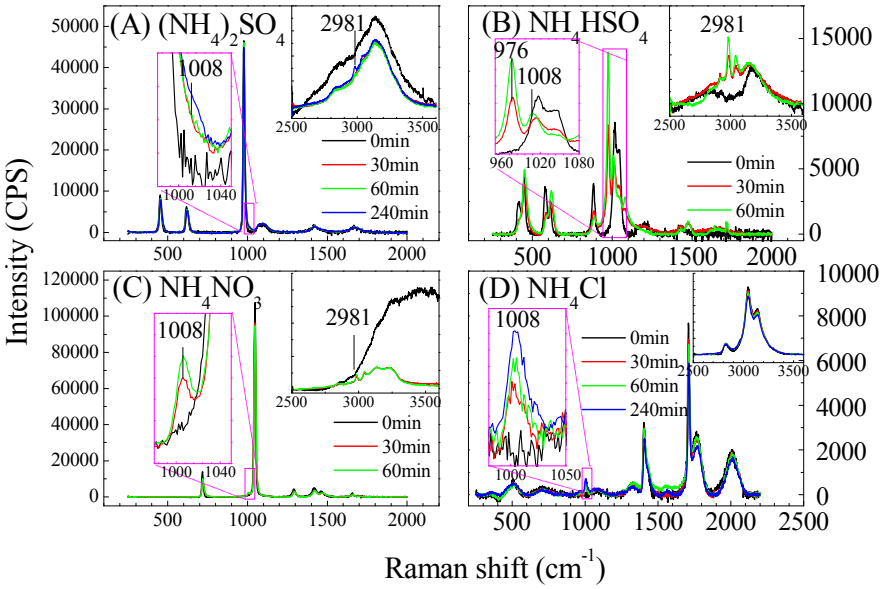

Fig. 2 *In situ* Raman spectra for heterogeneous reactions of MA with ammonium salts at 298 K. The insert graphs in purple boxes show the enlarged spectra in the range of 950-1080 cm^{-1} and those on the top right corner show the spectra in the range of 2500-3600 cm^{-1}.

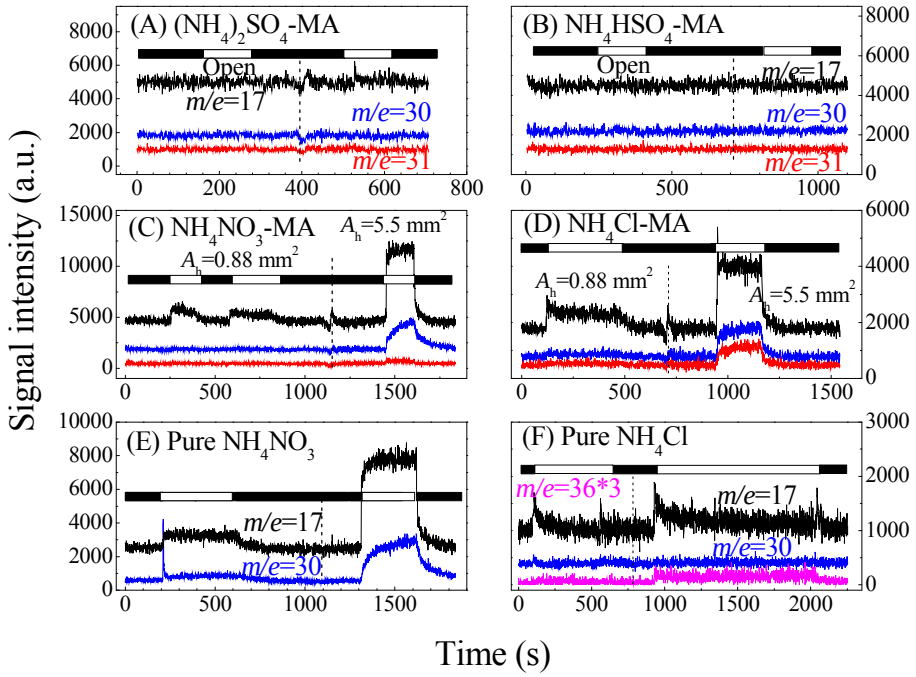

642

643 Figure 3. Desorption of surface species from MA treated salts and pure salts at 1.2 $\times 10^{-6}$ Torr

644 and at 298 K. (A) 58.2 mg $(NH_4)_2SO_4$, (B) 60.5 mg NH_4HSO_4, (C) 59.8 mg NH_4NO_3, (D)

645 63.9 mg NH_4Cl, (E) 59.8 mg pure NH_4NO_3 and (F) 60.5 mg pure NH_4Cl. The A_h is 0.88 mm^2

646 in left side of the dash lines, and it is 5.5 mm^2 in the right side of the dash lines.

647

648

649

650

651

652

653

654

655

656

657

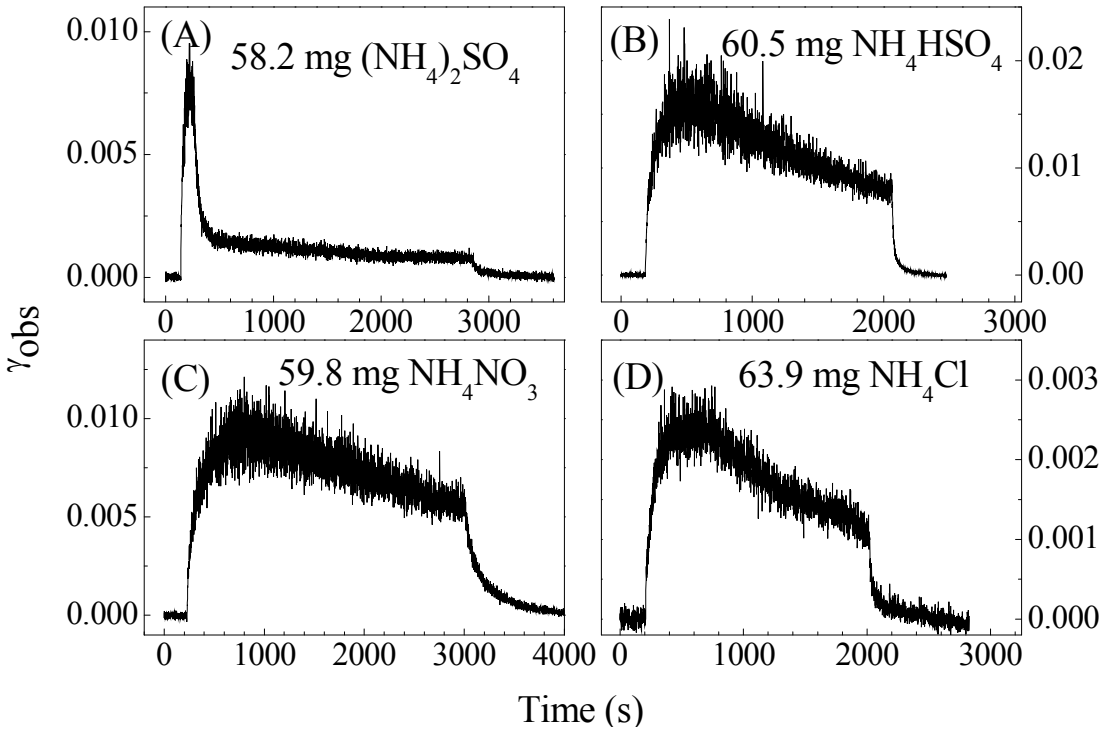

Fig. 4. Typical observed uptake coefficients of MA onto ammonium salts at 298 K.

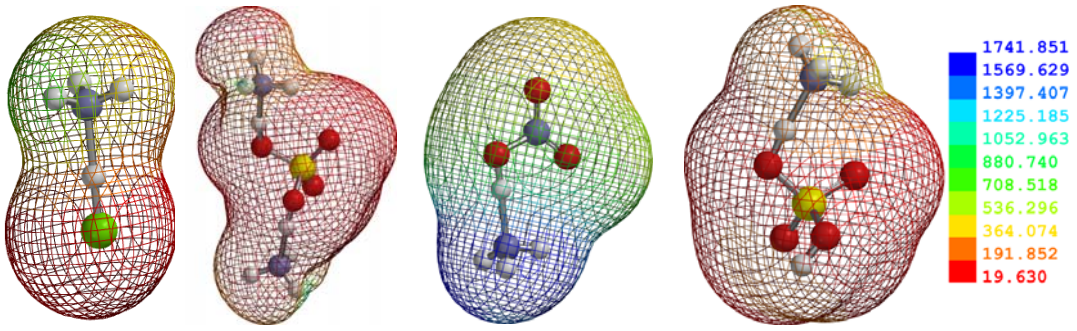

NH_4Cl **$(NH_4)_2SO_4$** **NH_4NO_3** **NH_4HSO_4**

Fig. 5. Electrostatic potential maps for ammonium salts.

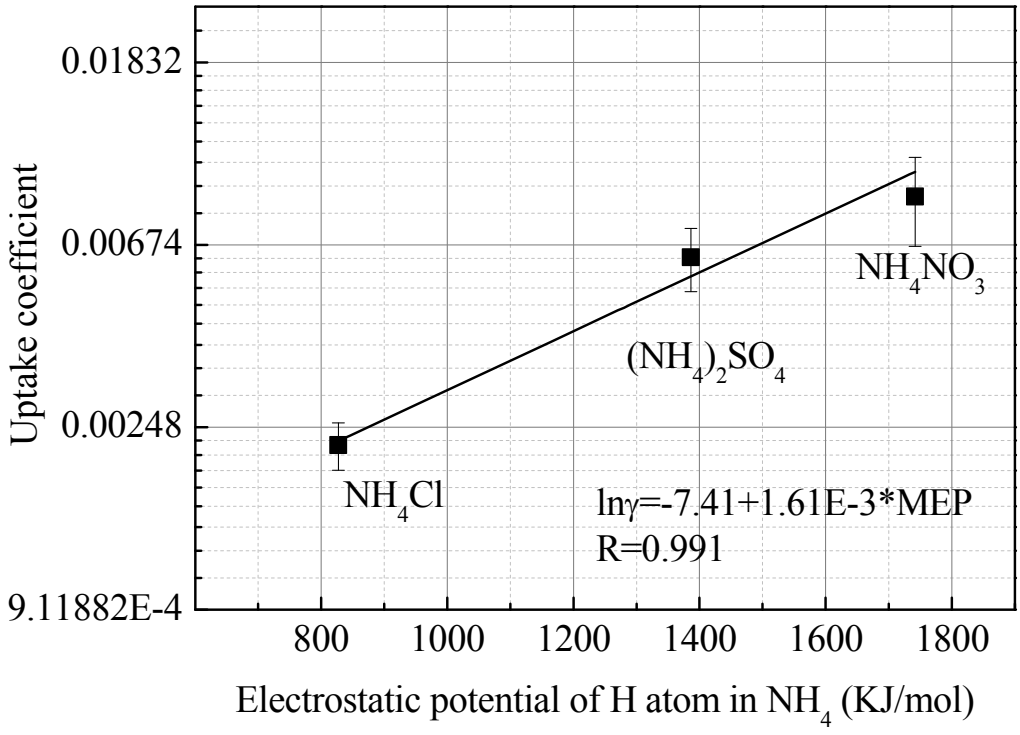

695

696 Fig. 6. Relationship between uptake coefficients of MA onto ammonium salts and the

697 electrostatic potential of H atom in NH_4^+.

698